PRETTY MISSION PREPARATIONS: STEPS TO FOSTER GRAZING-ANGLE REFLECTOMETRY

M. Semmling [1], W. Li [2], M. Hoque [1], J. Wickert [3,4], E. Cardellach [2], H. Fragner [5] H. Nahavandchi [6]

[1] German Aerospace Center (DLR), Institute for Solar-Terrestrial Physics, Neustrelitz, Germany
[2] Institute for Space Studies Catalunya (IEEC, ICE-CSIC), Barcelona, Spain
[3] German Research Centre for Geosciences (GFZ), Potsdam, Germany
[4] Technische Universität Berlin (TUB), Berlin, Germany
[5] Beyond Gravity Austria (BGA), Vienna, Austria
[6] Norwegian University of Science and Technology (NTNU), Trondheim, Norway

For the ESA mission PRETTY a three-unit cubesat is foreseen to be launched in March 2023. The satellite is designed for a low earth orbit (LEO) with a high inclination ($97.66°$), a low orbit excentricity and a mean orbit height of 564 km. The satellite layout comprises two scientific payloads: A passive reflectometer to acquire Earth-reflected signals of Global Navigation Satellite Systems (GNSS) and novel dosimeters to measure the Total Ionizing Dose (TID). This presentation concentrates on the preparation of the GNSS reflectometer measurements (reflectometry) for altimetric application over the global ocean and cryosphere. Reflectometry data from satellites have been used earlier for altimetric retrievals: over sea-ice [1], over the Caribbean [2] and the Seas of Indonesia [3]. The TDS-1 satellite mission and the CYGNSS constellation of reflectometry satellites were important milestones in this respect.

A crucial challenge for the altimetric application of reflectometry is the retrieval of precise observations over the global oceans. High precision in GNSS is achieved observing the carrier phase delay. Respective retrievals in reflectometry reach centimeter level precision, resolving sea surface topography [4]. This precise information, however, is lost over rough ocean areas due to the dominance of diffuse scatter and the absence of coherent reflection, see limitation in [2]. Group delay observations persist under diffuse scatter conditions. However, limits in code bandwidth and group delay sampling of the previous space-borne scenarios provided only meter-level precision (tracking error) [3].

The surface roughness and the observation geometry play an important role for the altimetric application. Reflectometry satellites often acquire signals in a near-nadir geometry (seen from the receiver) that corresponds to high elevation angles at the specular surface point (usually $> 45°$). High elevation angles imply a high altimetric sensitivity, however, they also imply a high sensitivity to surface roughness [5]. The PRETTY mission will shift the observation geometry to grazing angles with elevations between $5°$ and $15°$ at the specular point. This shift is expected to increase the number of coherent reflections and provide better conditions for carrier phase altimetry, as shown with airborne data [4].

PRETTY's focus on grazing angles is one step to mitigate the ocean roughness impact. The reduced height sensitivity in this case should still be sufficient to resolve decimeter-sized features of sea-surface topography, cf. simulations in [5] and feature detected in CYGNSS data [2]. The focus of the PRETTY mission on the L5 carrier frequency (1191.795 MHz) is another step to mitigate the ocean roughness impact. Compared to the commonly used L1 carrier (1575.42 MHz), L5 has a longer wavelength (lower frequency) and is more robust against roughness, cf. the Rayleigh criterion [6]. Finally, the interferometric concept of signal correlation is a third step of the PRETTY mission to improve altimetric precision. The reflected and the direct signal are correlated without using modelled replica of the signal. The interferometric approach can increase the bandwidth for group delay observations beyond the replica bandwidth. It may reach sub-meter precision in group delay waveforms [7].

The use of grazing-angle geometry and the use of L5 carrier are reasonable steps to explore altimetric retrievals. However, both steps increase the atmospheric delay that contributes to the error budget. Fig.1 shows three example events observed by the CYGNSS constellation that are analyzed, here, with respect to atmospheric biases.

All three events are at grazing-angle geometry with elevations between $12°$ and $15°$ at the specular point. Two of them date from September 2017, the third one from October 2018. They differ significantly with respect to local time at the specular point (around noon, in the evening and close to local mid-night). The local time spread and the low latitudes ($10°$ to $30°$ N in the Caribbean) causes variable atmospheric conditions. In particular, the ionospheric delay is expected to change significantly.

A dedicated simulation tool is used to compute delays induced by ionospheric refraction, neutral gas refraction and by an offset in surface height. Relative delays are provided: incoming ray (to the specular point) plus reflected ray (from the

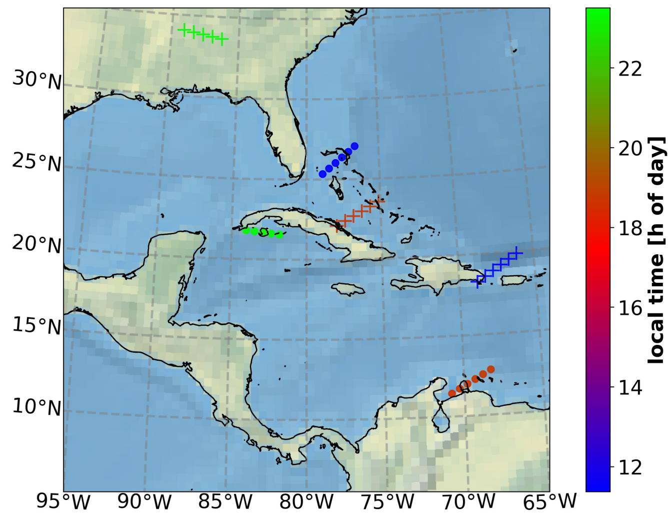

Fig. 1. Three reflection events in the Caribbean. Specular points (dots) and receiver ground tracks (crosses) are shown. Markers are color-coded with local time at the spec. point (about UTC-5h). The events refer to: GPS PRN 12 by CYG ID 4 on 2017/09/08 23h17 UTC (red); GAL PRN 1 by CYG ID 8 on 2017/09/20 16h37 UTC (blue) and GAL PRN 5 by CYG ID 5 on 2018/10/14 04h56 UTC (green).

	delay bias mag. [m]				delay residual mag. [m]			
	iono. L1	iono. L5	neut.	surf.	iono. L1	iono. L5	neut.	surf.
uncertainty	100%	100%	100%	10 m	10%	10%	1%	0.5 m
local noon event (blue)	10.6	18.3	18.3	5.3	1.1	1.8	0.2	0.3
local evening event (red)	9.0	15.8	20.8	4.5	0.9	1.6	0.2	0.2
local midnight event (green)	3.6	6.4	20.9	4.6	0.4	0.6	0.2	0.2

Table 1. Magnitudes of delays induced by ionosphere refraction on L1 and L5, neutral gas refraction and reflecting surface offset. Signs that distinguish phase and group delays are disregarded. Local time of the events refers to Fig. 1. Biases of total contributions (left columns). Residuals after correction with given uncertainty (right columns).

specular point) minus direct ray (to the receiver). The computed ionospheric part is based on the empirical Neustrelitz Electron Density Model (NEDM) [8]. The neutral gas part assumes standard atmosphere conditions [9] to account for tropospheric and stratospheric refraction. A surface height offset of 10 m is assumed to compute a related delay bias, typical for geoid undulations at the ocean surface. A residual offset of 0.5 m (after geoid correction) is then assumed for the effect of remaining sea surface topography. Table 1 shows the results of delay biases and corresponding residuals assuming model correction with dedicated uncertainties.

We conclude from the results that delays of neutral gas and ionosphere have major impact. The ionospheric delay is especially important as even the residual after model correction still reaches the meter scale. An important goal for PRETTY is to improve the precision, especially of group delays, to sub-meter level, as explained in [7]. Then, the observations can be valuable either to advance altimetric retrievals or monitor the ionospheric electron content.

1. REFERENCES

[1] W. Li, E. Cardellach, F. Fabra, A. Rius, S Ribó, and M. Martín-Neira, "First Spaceborne Phase Altimetry over Sea Ice Using TechDemoSat-1 GNSS-R Signals," *Geophys. Res. Lett.*, vol. 44, pp. 8369–8376, 2017.

[2] E. Cardellach, W. Li, A. Rius, M. Semmling, J. Wickert, F. Zus, C. Ruf, and C. Buontempo, "First precise spaceborne sea surface altimetry with GNSS reflected signals," *IEEE JSTARS*, vol. 13, pp. 102–112, 2019.

[3] J. Mashburn, P. Axelrad, C. Zuffada, E. Loria, A. O'Brien, and B. Haines, "Improved GNSS-R Ocean Surface Altimetry With CYGNSS in the Seas of Indonesia," *IEEE Trans. Geosci. Rem. Sens.*, vol. 58, no. 9, pp. 6071–6087, 2020.

[4] A. M. Semmling, J. Beckheinrich, J. Wickert, G. Beyerle, S. Schön, F. Fabra, H. Pflug, K. He, J. Schwabe, and M. Scheinert, "Sea surface topography retrieved from GNSS reflectometry phase data of the GEOHALO flight mission," *Geophys. Res. Lett.*, vol. 41, pp. 954–960, 2014.

[5] A. M. Semmling, V. Leister, J. Saynisch, F. Zus, S. Heise, and J. Wickert, "A phase-altimetric simulator: studying the sensitivity of Earth-reflected GNSS signals to ocean topography," *IEEE Trans. Geosci. Rem. Sens.*, vol. 54, no. 11, pp. 6791–6802, 2016.

[6] P. Beckmann and A. Spizzichino, *The Scattering of Electromagnetic Waves from Rough Surfaces*, Artech House, Inc., Nordwood, MA, 1987, Reprint. Originally published: Oxford [Oxfordshire]; New York : Pergamon Press, 1963. (International Series of Monographs on Electromagnetic Waves; 4).

[7] E. Cardellach, A. Rius, M. Martín-Neira, F. Fabra, O. Nogués-Correig, S. Ribó, J. Kainulainen, A. Camps, and S. D'Addio, "Consolidating the Precision of Interferometric GNSS-R Ocean Altimetry Using Airborne Experimental Data," *IEEE Trans. Geosci. and Remote Sens.*, vol. 52, pp. 4992–5008, 2014.

[8] N. Jakowski and M. M. Hoque, "A new electron density model of the plasmasphere for operational applications and services.," *J. Space Weather Space Clim.*, vol. 8, pp. A16, 2018.

[9] ISO, "Standard Atmosphere," *International Organization for Standardization*, vol. 2533:1975, 1975.